

# Plasma-assisted CO<sub>2</sub> hydrogenation over Ni-zeolite catalysts under vacuum

D. Bento<sup>a\*</sup>, F. Azzolina-Jury<sup>b</sup>, C. Henriques<sup>a</sup>, F. Thibault-Starzyk<sup>b</sup>

<sup>a</sup> CQE, Centro de Química Estrutural, Instituto Superior Técnico, Universidade de Lisboa, Av. Rovisco Pais, 1049-001 Lisboa, Portugal

<sup>b</sup> Laboratoire Catalyse et Spectrochimie, CNRS-ENSICAEN-Université de Caen. 6 boulevard du Maréchal-Juin, 14050 Caen, France

\* Corresponding author: diogobento@tecnico.ulisboa.pt

---

## Abstract

Ni-impregnated CBV and ZSM-11 catalysts were prepared with different amounts of metal and by different impregnation methods for application on the CO<sub>2</sub> hydrogenation reaction. Their characterization was performed by determining their external and internal surface areas, micro- and mesopores volume, crystallinity, reduced Ni fraction on the catalyst and by analyzing SEM images of each sample. All the analyzed catalysts revealed crystallinity above 99%. Crystal sizes of 250 for ZSM-11 and 500 for CBV zeolites were obtained. The H<sub>2</sub>TPR-MS method was used to determine the reduced Ni level of each sample in-situ. The hydrogenation reaction was performed in a packed-bed reactor under vacuum under conventional heating and plasma-assisted conditions. The activity of each sample was found to be influenced by the nickel amount and reduction level on the catalyst. The reaction was also performed under two different plasma-catalytic configurations at different volumetric flows: In-plasma catalysis (IPC) and Post-plasma catalysis (PPC), with the first presenting the highest activity. The results were found to be influenced by the residence time of the gas in plasma as well as by the interaction between plasma and catalyst. An unreported phenomenon was verified while performing the IPC reaction. The plasma induced enhancement of the catalyst adsorption capacity, resulting on methane storage during plasma activity and its release upon plasma's extinction. This occurrence was evidenced by IR measurements that were performed during and after plasma.

*Keywords:* CO<sub>2</sub>, Hydrogenation, Methanation, Plasma, Zeolite, Catalysis

---

## 1. Introduction

Since the end of the industrial revolution, after the XIX century, the energetic needs across the world have been increasing. Due to this augmentation, and the consequent growth of the fuel prices, the interest about renewable energy sources has been rising, in particular since the end of 2004 [1]. Nevertheless, these kinds of energy sources, due to disadvantages such as high development cost, unavailability in certain areas, inability of large quantity production or difficulty in energy storage, are still not as reliable as like fossil fuel resources such as petroleum or coal [2].

The excessive use of fossil fuels consequences include the release of abnormal quantities of carbon dioxide as well as of pollutants such as sulfur, carbon and nitrogen oxides, contributing to air, land and water pollution. A very well-known consequence of these emissions is the greenhouse effect which contributes to the global warming phenomenon [3].

It is then important to research and develop technologies that allow us to produce energy efficiently from clean and preferably renewable sources.

The CO<sub>2</sub> hydrogenation reaction allows its conversion into compounds such as CH<sub>4</sub>, which can be used as

synthetic natural gas (SNG) and applied as a fuel in energy power plants, or as CO, which together with H<sub>2</sub> makes synthesis gas (syngas) that can be converted to hydrocarbons, olefins, paraffin, alcohols, ketones, acids or aldehydes by the Fischer-Tropsch reaction.[4]

Catalysts based on metals from group VIII such as Ru, Rh and Pd have been studied in the CO<sub>2</sub> hydrogenation field. Ni-based catalysts tend to be preferred due exhibiting a similar performance to that of these metals and having a fairly lower cost [5,6].

The hydrogenation reaction has been carried, mostly at atmospheric pressure and within temperature ranges of 200 to 500°C[3, 7-8].

The application of non-thermal plasma (NTP) to this reaction has been studied by [1]. It has been verified that NTP enhances the dissociation of CO<sub>2</sub>, creating reactive species and promoting its hydrogenation[1].

In this work, plasma-assisted CO<sub>2</sub> hydrogenation was compared with the conventional heating reaction in a packed-bed reactor. Ultra-stable Y (USY) and ZSM-11 catalysts with different Si/Al ratios and Ni content were used under high vacuum and temperatures between 200 and 450°C. *Operando* infrared (IR) measurements were performed with an USY catalyst, during and after plasma

activity, in order to gather more information about its influence in the reaction.

## 2. Experimental procedures

### 2.1. Catalysts preparation

The catalysts used in this work were previously synthesized and were prepared by two distinct impregnation methods. 14 wt.% of nickel was introduced on two USY samples supplied by Grace Davison by two different impregnation methods: wet impregnation (Imp) and incipient wetness impregnation (IWI). The remaining samples were previously impregnated with their impregnation methods and nickel amounts summed in table 1.

**Table 1 - Impregnation method and Ni content of each catalyst.**

Catalyst	Impregnation method	Ni wt.%
Ni/USY(30)	Wet Impregnation	14
Ni/USY(40)	Wet Impregnation	14
Ni/USY(40)	Incipient Wetness Impregnation	14
Ni/ZSM-11	Wet Impregnation	2.5
Ni/ZSM-11	Wet Impregnation	5

Before the reactions every catalyst sample was submitted to a calcination step by heating each sample under air until 500°C with a heating rate of 10°C/min under and holding this temperature for 3 hours.

### 2.2. Catalysts characterization

The CBV and ZSM-11 catalysts crystallinity was analyzed by X-ray diffraction (XRD) with a PANalytical X'Pert PRO diffractometer with CuK $\alpha$  radiation ( $\lambda=0.15418$ , 40 mA, 45 kV). The diffraction of these two zeolites was collected in  $2\theta=5-60^\circ$  and  $2\theta=5-50^\circ$ , respectively with increments of  $0.1^\circ$  and at a rate of  $2^\circ/\text{min}$  [9].

The internal and external surface areas and micro- and meso-porous volume were determined at 77K by N<sub>2</sub> adsorption-desorption using the Brunauer-Emmet-Teller (BET) method. A Micromethrics sorptometer Tri Star 3000 was used for this effect [9].

Scanning electron microscope (SEM) pictures of these samples were also obtained by using a SEM with 30 kV of acceleration voltage. [9]

Before every reaction, every catalyst sample was dried and submitted to an *in-situ* reduction step by hydrogen temperature-programmed reduction followed by mass spectroscopy (H<sub>2</sub>TPR-MS). The drying step was performed under a flow of 30 mL/min of N<sub>2</sub> and a pressure of 2.4 Torr,

heating each sample from room temperature to 200°C at a rate of 10°C/min and holding this temperature for 45 minutes. The reduction was carried out with the same volumetric flow and pressure, using a mixture composition of 5% H<sub>2</sub>/N<sub>2</sub>. The temperature was increased from room temperature to 470°C with a heating rate of 10°C/min and then held for 3 hours.

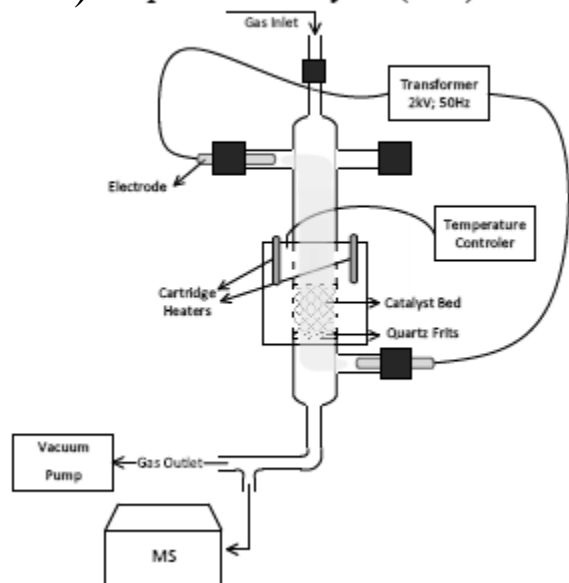
### 2.3. Catalytic tests

#### 2.3.1. Packed-bed reactor

The CO<sub>2</sub> hydrogenation reaction was studied within a Pyrex® packed-bed tube reactor with 2 cm of inner diameter and 12 cm of height. The reactor is filled with 1.2g of catalyst in the form of pellets with approximately 3 mm of diameter and 1 mm of thickness supported by a quartz frit. Two tungsten electrodes are coupled to the reactor and connected to a high voltage ac power supply (2 kV, 50Hz) in order to generate a glow-discharge plasma across the catalyst bed. The reactional mixture is sent to the packed-bed by the top of the reactor, which is connected to a gas-system including gas flow controllers (Brooks). The outlet of the reactor is connected to a Quadrupole Mass Spectrometer (Pfeiffer Omnistar GSD 301) and to a vacuum pump. A heating jacket connected to an EROelectronic temperature controller was equipped to the reactor in order to carry the reaction under different temperatures. The packed-bed reaction was performed with the CBV and ZSM-11 samples under conventional heating, between 200 and 450°C and plasma-assisted heating between 125 and 350°C. A volumetric flow of 20 mL/min was fed to the reactor with a molar ratio of H<sub>2</sub>/CO<sub>2</sub>/Ar=4/1/5. Under these conditions, a pressure of approximately 2 Torr was obtained.

In a second stage, a plasma-catalyst interaction study was performed by comparing the catalytic activity of the Ni/USY(40) sample under two different reactional configurations: In-plasma catalysis (IPC) and Post-plasma catalysis (PPC), as shown in figure 1. In the IPC configuration the catalyst is in direct contact with the plasma, while in the PPC configuration, the reactional mixture will be submitted to plasma before reaching the catalyst and after sent to the packed-bed. This set of experiments was performed under 125°C (NTP's temperature) with a feeding stream with a volumetric flow from 10 to 100 mL/min, having the same molar composition as the previous experiments.

### a) In-plasma catalysis (IPC)



### b) Post-plasma catalysis (PPC)

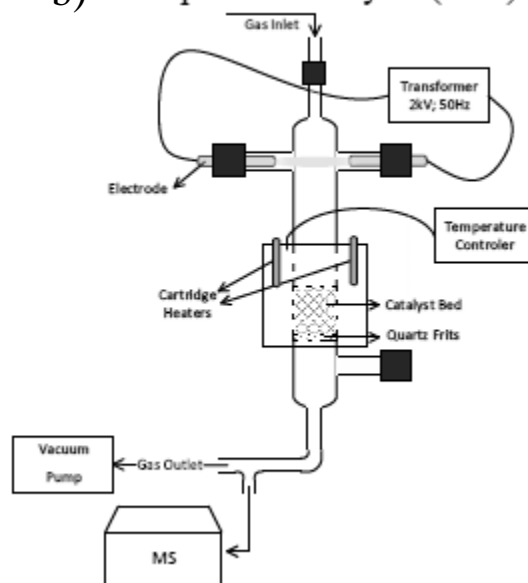


Figure 1 – a)IPC configuration; b)PPC configuration

#### 2.3.2. Operando IR Measurements

Operando IR Measurements were also performed using this catalyst during and after plasma in a Bruker Vertex 80v FTIR spectrometer. The IR spectra were acquired between 4000 and 1000  $\text{cm}^{-1}$  with a resolution 16  $\text{cm}^{-1}$ . These measurements were conducted on a static IR-cell schematized in figure 2, during and after plasma-assisted  $\text{CO}_2$  hydrogenation.

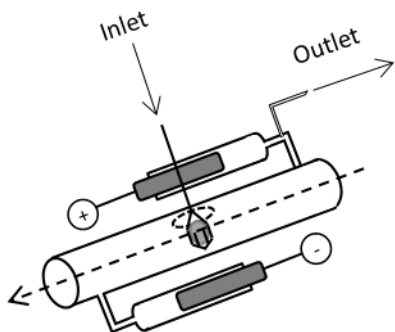


Figure 2 – Static IR cell scheme.

## 3. Results and Discussion

### 3.1. Catalysts characterization

The XRD measurements performed for each catalyst revealed that the crystalline structure of every sample was over 99% of the total structure and it was not found to be affected throughout this work.

In Table 2 are summed the results obtained for the crystallinity, silica/alumina molar ratio, nickel content and its reduction level, internal and external surface area as well as microporous and mesoporous volume of each one of the analyzed samples. Characteristics such as micro- and mesopores volume and internal and external surface areas seem to be related with the framework type of each zeolite as well as with the to decrease with the increase of the Si/Al molar ratio. In [9], F. Azzolina-Jury explains that a higher alumina content in nickel content of each sample. The pore volume was found the framework leads to an increase of the negative charge in the zeolite which promotes the hostage of  $\text{Ni}^{2+}$  ions in its exchangeable sites. A greater amount of these ions in the zeolites structure leads to a decrease of the internal surface area and the consequent diminution of the micropore volume of the zeolite. This also affects the reduced Ni values since the reduction of  $\text{Ni}^{2+}$  requires higher temperatures than those necessary to reduce NiO [9]. This justifies why ZSM-11 catalysts, in general, exhibit lower internal surface area and both micro- and mesoporous volume, and why USY(40), with lower alumina content, presents the highest values for these properties. Between the two ZSM-11 samples, the difference in values is due to the Ni amount of each catalyst. As the nickel content of a catalyst increases, the  $\text{Ni}^{2+}$  amount hosted in the zeolite will naturally also increase. The external surface area difference between each sample can be associated to the particle size of each catalyst sample which is influenced by the respective zeolite type.

**Table 2 – Catalyst samples characterization.**

Zeolite	Crystallinity (%)	Si/Al Ratio (mol)	Ni content (% wt)	Ni <sup>o</sup> <sub>frac</sub> (%)	Internal surface area (m <sup>2</sup> /g)	External surface area (m <sup>2</sup> /g)	Micropores volume (cm <sup>3</sup> /g)	Mesopores volume (cm <sup>3</sup> /g)
USY(30)	>99%	30	14.0	13.4	513	106	0.197	0.201
USY(40)	>99%	40	14.0	17.4	632	107	0.252	0.201
USY(40)(IWI)	-	40	14.0	24.3	-	-	-	-
ZSM-11	>99%	17	5.0	6.6	252	57	0.085	0.154
ZSM-11	>99%	17	2.5	16.6	291	69	0.107	0.195

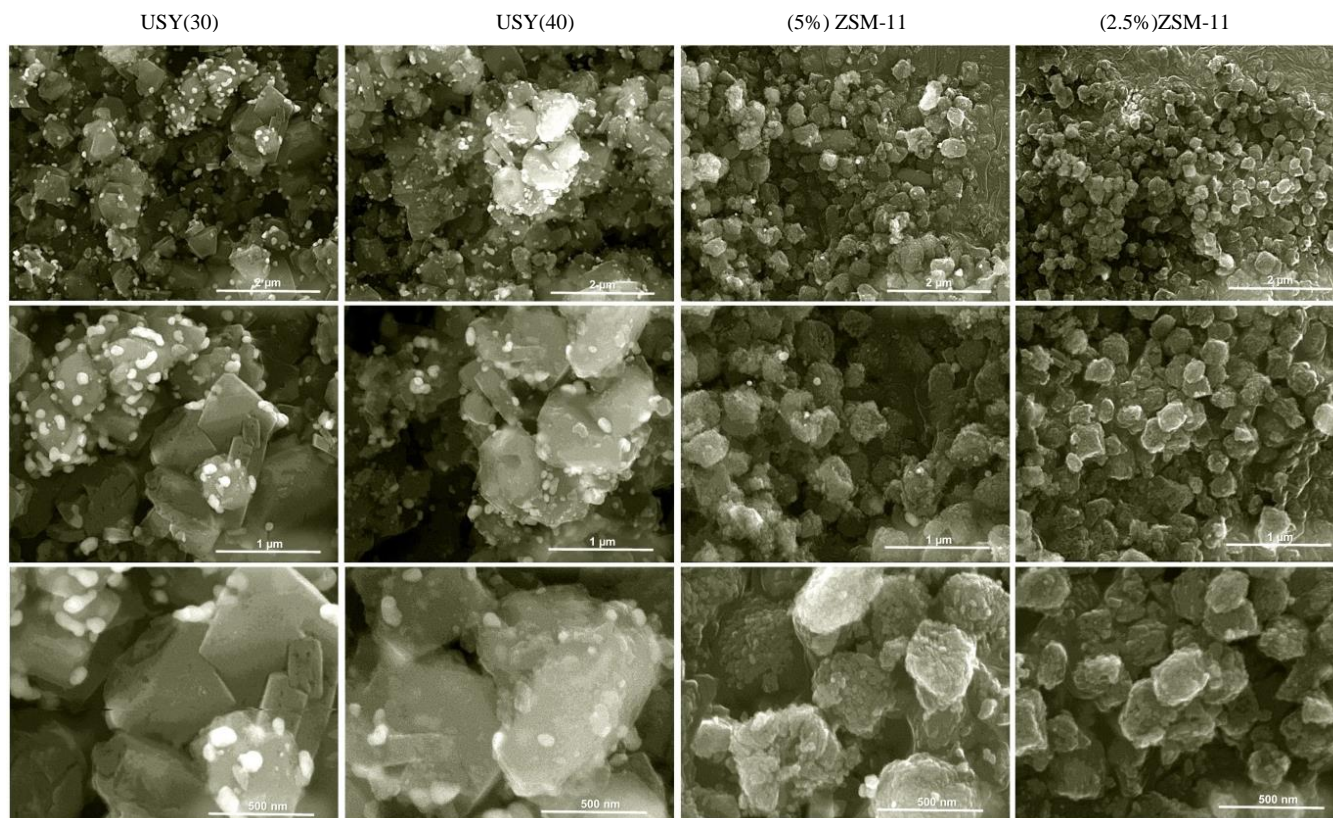
The images obtained from the scanning electron microscopy (figure 3) puts in evidence the size of the zeolite crystals of each catalyst sample. The USY samples, which are based on FAU zeolites, have crystals with a size of nearly 500 nm. ZSM-11 catalysts, based on MEL zeolites, seem to have smaller crystals with sizes of approximately 250 nm. These values match with the lower external surface area obtained for the USY catalysts. Nickel agglomerates with approximately 50 nm can be seen in these images, being especially noticeable in the USY catalysts due to the higher Ni content of these samples. The agglomerate density on the images is directly related with the Ni amount in each sample [9].

Based on the *in-situ* reduction hydrogen consumption profiles for each catalyst sample it was determined the Ni amount on the catalyst that was reduced (Ni<sup>o</sup><sub>frac</sub>).

The results obtained through the H<sub>2</sub>TPR-MS experiments are summed in Table 2.

The higher amount of reduced nickel of the USY(40) sample in comparison to that of USY(30) can be explained by the higher alumina content of this last, leading to a higher amount of Ni in its ionic form (Ni<sup>2+</sup>) which requires higher temperatures to be reduced [11]. The USY(40) impregnated with the IWI method presents a higher Ni<sup>o</sup><sub>frac</sub> than the sample of the same zeolite prepared by wet impregnation since the IWI method allows a better dispersion of the Ni particles through the catalyst. As the ZSM-11 samples have the same Si/Al ratio, the different Ni<sup>o</sup><sub>frac</sub> values are attributed to the higher Ni content of the 5 wt.% Ni sample which leads to a greater amount of Ni<sup>2+</sup> species and consequent lower reduction.

**Figure 3 – SEM images of the USY and ZSM-11 samples.**



### 3.2. Catalytic tests

#### 3.2.1. Packed-bed reactor

The results obtained during the CO<sub>2</sub> hydrogenation reaction within the packed-bed reactor are presented in Figures 4,5 and 6. The CO<sub>2</sub> conversion ( $CO_2Conv$ ), selectivity ( $S_i$ ) and yield ( $Y_i$ ) towards a product as well as the carbon balance to the reactor ( $C_{balance}$ ) were calculated by applying the following expressions.  $CO_{2in}$  and  $CO_{2out}$  are the amounts of CO<sub>2</sub> that enter and leave the reactor, respectively.  $i_{produced}$  is the produced amount of a product  $i$ .  $n_{Cin}$  and  $n_{Cout}$  express the molar amount of carbon that is sent and leaves the reactor, respectively.

$$CO_2Conv = \frac{CO_{2in} - CO_{2out}}{CO_{2in}} \times 100\% \quad (1);$$

$$S_i = \frac{i_{produced}}{CO_{2in} - CO_{2out}} \times 100\% \quad (2);$$

$$Yield_i = \frac{i_{produced}}{CO_{2in}} \times 100\% = CO_2Conv(\%) \times S_i(\%) \quad (3);$$

$$C_{balance} = \frac{n_{Cout}}{n_{Cin}} \times 100\% \quad (4)$$

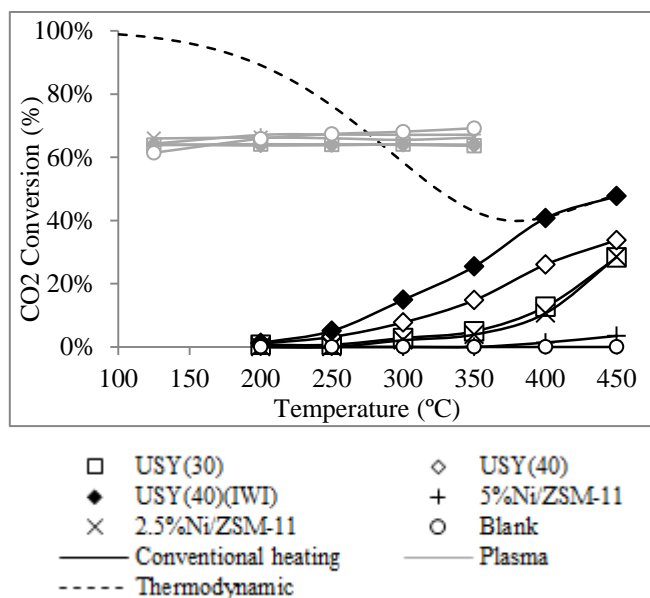


Figure 4 – CO<sub>2</sub> Conversion vs temperature results.

Under conventional heating, within the temperature range studied, the CO<sub>2</sub> conversion was found to increase with heating. The performance of each catalyst in the dissociation of CO<sub>2</sub> seemed to be related with the amount of reduced Ni on the catalyst, with USY(40)(IWI) presenting the higher conversion values, followed by USY(40), USY(30), 2.5%Ni/ZSM-1 and 5%Ni/ZSM-11 with a very low activity. The Ni<sup>0</sup> species on the surface of catalysis allow the dissociative adsorption of hydrogen, which facilitates the dissociation of CO<sub>2</sub> and its further hydrogenation [9]. The blank experiment does not reveal

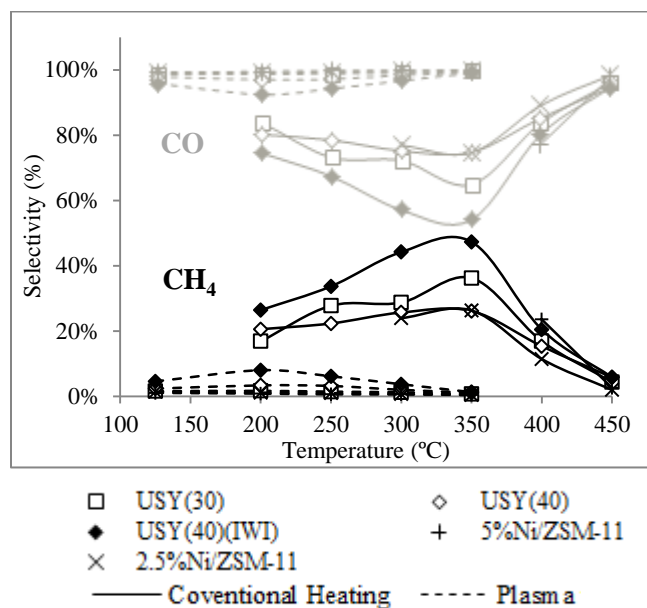


Figure 5 – Selectivity towards CH<sub>4</sub> and CO.

any conversion from 200 to 450°C. These values tend to be closer to the thermodynamical limit as the temperature increases as a consequence of the higher thermal activation of the catalyst. When the reaction is carried under plasma-assisted heating, the CO<sub>2</sub> conversion increases significantly for every catalyst sample as well as when no catalyst is used. In this case the carbon dioxide is thought to dissociate in the gas phase by ionization due to the plasma discharge instead of being converted in the catalyst. The fact of similar conversion values being achieved for every catalyst samples (60-70%), as well as in the blank experiment supports this affirmation. In this case, temperature does not seem to have such a strong influence as in the conventional heating hydrogenation, since the CO<sub>2</sub> is dissociated by plasma-induced ionization. It was also verified that unlike the conventional heating experiments results, slightly higher conversion values were obtained with the ZSM-11 catalysts, despite their lower Ni content and Ni<sup>0</sup><sub>frac</sub> in the case of the sample with 5wt.% Ni. Also, it was found that as the temperature increases the blank experiment tends to achieve greater CO<sub>2</sub> consumption than the experiments with catalysts. The increasing conversion values for the blank experiment can be explained by the temperature enhancement of plasmas energy which leads to a higher CO<sub>2</sub> ionization. The difference of conversion results verified for the ZSM-11 and USY catalysts can be explained by plasma-catalyst interactions and recurring to the complex permittivity values of the zeolites. These interactions are thought to consume part of plasmas energy leading to less energy being applied to the ionization of carbon dioxide, which causes its lower conversion value. As suggested by F. Azzolina-Jury in [9], FAU zeolites



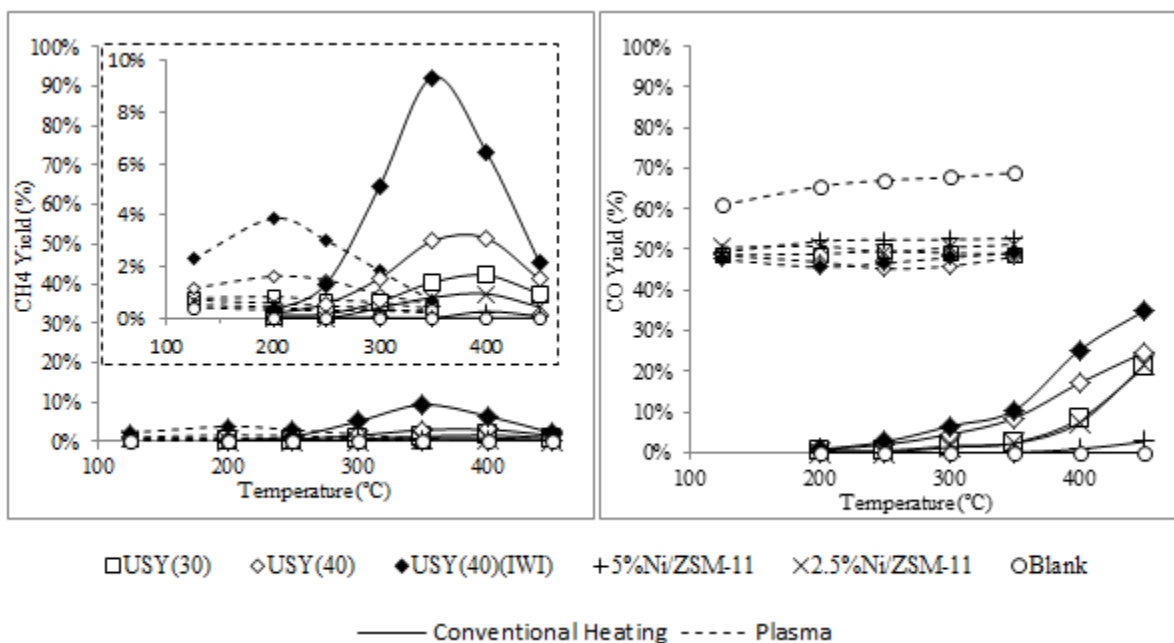


Figure 6 – CH<sub>4</sub> (a) and CO (b) Yield vs temperature for each catalyst sample.

possess higher complex permittivity values than MEL zeolites, indicating that the electric field and plasmas effect on the zeolite has a higher importance, leading to the lower CO<sub>2</sub> observed for the USY catalysts [9]. Plasma-assisted CO<sub>2</sub> conversion achieved values that overcome the thermodynamical limits for higher temperatures (above 300°C) due to the great variety of high-energy species that are created by plasma-ionization of the gases in the reactional mixture.

Looking for the results in terms of selectivity, in the conventional heating case, the better methane selectivity achieved with the USY, especially USY(40)(IWI), catalysts can once again be attributed to the higher Ni<sup>0</sup> amount on the surface of the catalyst that, due to allowing a greater amount of hydrogen to be adsorbed, facilitates the hydrogenation of the dissociated CO into CH<sub>4</sub>. Besides the Ni<sup>0</sup> effect, the structure of the zeolite appears to have a significant influence on the selectivity of the reaction. ZSM-11 catalysts, especially 2.5%Ni/ZSM-11, despite having a much lower Ni<sup>0</sup> content, achieved CH<sub>4</sub> selectivity values very close to the ones obtained with USY(30). The selectivity towards methane can be linked to the adsorption capacity of a catalyst. Under conventional heating operation, the hydrogenation of the dissociated CO<sub>2</sub> molecules into CH<sub>4</sub> depends on its adsorption and interaction with the hydrogen that is adsorbed in the metallic nickel of the catalyst. For every catalyst sample the selectivity towards methane reached its maximum at 350 °C. To explain this maximum it must be considered that the selectivity of the reaction is influenced by an equilibrium between the temperature influence in two factors: a) the CO dissociation on the catalyst, b) the adsorption-desorption

equilibrium that was reported to be the rate determining step of this reaction [1,9]. Below 350°C the factor a) assumes a greater significance, being noticeable an increase of the CH<sub>4</sub> selectivity with the temperature. After 350°C the high temperature, together with the low pressure in the reactional system, make b) more relevant. This cause the premature desorption of the species in the catalyst, not allowing the hydrogenation of CO into CH<sub>4</sub> [9]. During the plasma-assisted reaction, a similar behavior is noticed, with the maximum CH<sub>4</sub> selectivity being achieved at 200°C. This peak can be justified the same way the one of conventional heating was. The better behavior exhibited by the USY zeolites in terms of plasma-assisted methane selectivity can be explained by the plasma-catalyst interaction mentioned before. It is thought that plasmas contact with the catalyst causes an enhancement of its adsorption capacities [12]. As the FAU zeolites have higher complex permittivity values, they are strongly affected by the NTP discharge and suffer a greater adsorption capacity enhancement, which allows achieving greater CH<sub>4</sub> selectivity values [9]. As the only products identified during the experiments were CH<sub>4</sub> and CO, the selectivity towards this last compound was assumed as  $S_{CO}=1-S_{CH_4}$ .

The yield of the reaction towards the two products was calculated as a product between the CO<sub>2</sub> conversion and the respective products selectivity. For both conventional heating and the plasma-assisted reaction the catalyst which revealed to have the highest CH<sub>4</sub> yield was 14%Ni/USY(40) (IWI), followed by 14%Ni/USY(40), 14%Ni/USY(30), 2.5%Ni/ZSM-11 and 5%Ni/ZSM-11. Despite plasma revealing a greater CO<sub>2</sub> conversion potential, in steady-state operation, its optimal methane

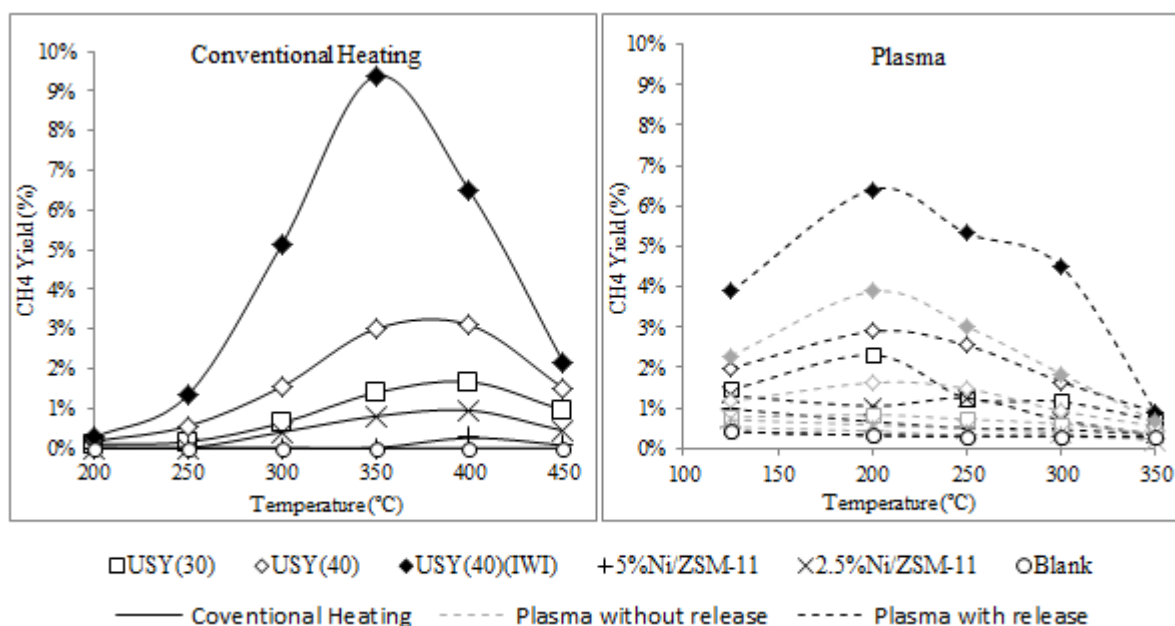


Figure 8 – Methane yield under conventional heating and plasma-assisted reaction for each catalyst considering the release.

yield was not found to surpass the one achieved through conventional heating. However, when the NTP is used the optimal temperature suffers a shift from 400°C to 200°C, and at this last temperature plasmas results surpass the ones achieved with only thermal power.

### 3.2.2. Plasma-induced methane release phenomenon

During the plasma-assisted experiments an unreported phenomenon was observed. After plasma operation, upon plasmas extinction, a sudden increase on CH<sub>4</sub> MS signal would be detected while every other reactant or products signal would return to its original value. An example of this behavior is shown in Figure 7.

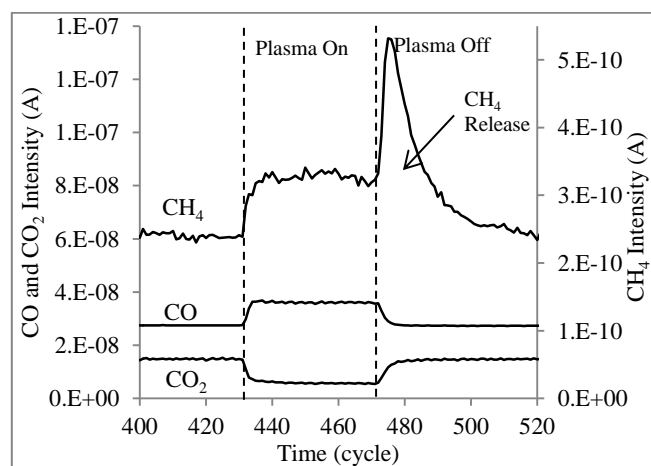


Figure 7 – Example of the methane release.

This occurrence suggests that some CH<sub>4</sub> or its radicals are being trapped/stored in the catalyst during plasma

activity due to the plasma-enhanced adsorption capacity. After the discharge extinguishes these radicals can react with the hydrogen which is adsorbed in the Ni<sup>0</sup> to form CH<sub>4</sub>. As methane is a non-polar molecule, under normal conditions it is not adsorbed in the zeolite. Then, due to the high temperature and low pressure inside the system it desorbs from the catalyst, being detected by the MS.

In order to proof this theory the carbon balance of the reactor was calculated according with equation 4. Before the methane release the carbon balance was found to be incomplete, closing after the release being considered in the quantification of the products. This supports the idea that some product is being retained in the zeolite during plasma operation. Then, re-doing the calculations of the reactions yield considering this amount of CH<sub>4</sub> the results presented in Figure 8 are obtained.

The new results reveal a significant increase in CH<sub>4</sub> yield comparing with the ones presented in Figure 6. The optimal temperature values for plasma-assisted operation (200°C) are now high enough to surpass the ones obtained under conventional heating at 400°C (with the exception of the most active sample). And they largely surpass the values obtained at 200°C with only thermal activity.

### 3.3. Operando IR Measurements

In order to analyze the adsorbed species on the zeolite IR spectra were taken with the USY(40) sample during and after the plasma-assisted reaction. Figure 9 shows the results of these measurements.

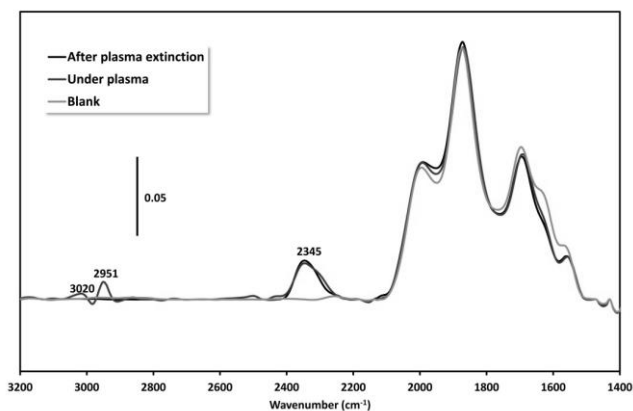


**Figure 9 – IR spectra during and before plasma activity.**

The bands observed under plasma at 3020 and 2951  $\text{cm}^{-1}$  correspond to the  $\nu_3$  antisymmetric C-H stretching mode of free and adsorbed methane, respectively, put in evidence that there is partial adsorption of methane or its radicals in the catalyst during plasma activity. These bands are not identified in the spectrum after plasma, suggesting that  $\text{CH}_4$  desorbs quickly after its extinction. The band at 2345  $\text{cm}^{-1}$  corresponds to the asymmetric stretching vibration of  $\text{CO}_2$  [9]. When the discharge is taking place it is noticed that this bands intensity decreases due to the conversion of this compound.

### 3.4. In-plasma vs Post-Plasma catalysis

The  $\text{CO}_2$  hydrogenation reaction was carried out with two different packed-bed plasma-catalytic configurations: IPC and PPC. The results obtained are shown in figures 10, 11 and 12.

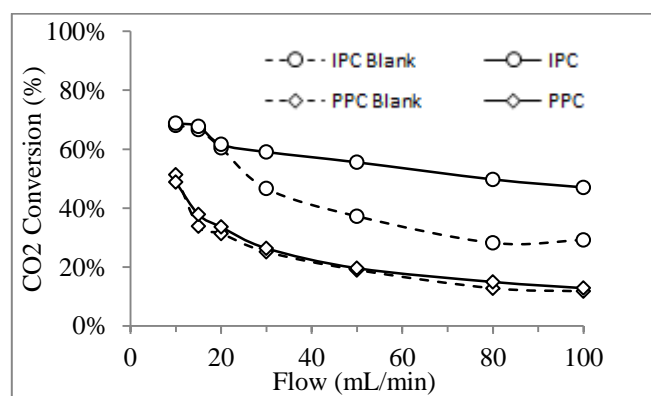


**Figure 10 –  $\text{CO}_2$  Conversion vs flow results for IPC and PPC.**

In terms of  $\text{CO}_2$  conversion the IPC system reveals to be clearly superior to PPC (with or without catalyst). This relies on the fact that, under plasma operation, the  $\text{CO}_2$  conversion occurs mainly in the gaseous phase due to plasma-induced ionization. In the IPC configuration, the plasma volume ( $\approx 25.1 \text{ cm}^3$ ) is much higher than that of

PPC configuration ( $\approx 3.1 \text{ cm}^3$ ). This causes a higher residence time of the reactional mixture in plasma which justifies the greater conversion of carbon dioxide obtained in the first configuration. In IPC the residence time in plasma was found to vary between 73 to 232 ms while in PPC it ranged from 9 to 29 ms according with the volumetric flow used (from 10 to 100 mL/min). This is supported by the decrease of conversion with the increase of volumetric flow. Both configurations presented higher conversion values with catalyst than without it, evidencing the catalysts importance in the conversion of  $\text{CO}_2$  even when plasma is used. In the IPC configuration, between 20 and 30 mL/min, a change of behavior of the  $\text{CO}_2$  conversion vs flow profile is noticed. This is explained in [9] as a consequence of a compromise between the effect of the increase of the volumetric flow in: a) the diminution of the residence time of the gas in plasma, and b) the enhancement of the reactions rate by sending more short lifetime reactive species created by plasma into the catalyst. Between 10 and 20 mL/min a) seems to have bigger relevance, since the  $\text{CO}_2$  conversion drops faster as the flow increases. Between 20 and 30 mL/min the conversion becomes constant, suggesting that these two factors reach a similar importance. Beyond 30 mL/min the b) becomes more relevant than a) changing the slope to a slight decrease with the flow increase. This suggests that after this flow the reaction mechanism changes as a consequence of the highly reactive species that are sent into the catalyst. These species are more easily adsorbed on the catalysts surface and may provide different kinds of interactions with other molecules or species. Looking into selectivity and yield results a similar behavior can be observed, which relies on the same reason [9].

IPC was found to surpass PPC in terms of  $\text{CO}_2$  conversion as well as yields of both products. This better performance is due to two main reasons. The first being the already referred greater residence time of the gas in plasma and the second the fact that in IPC plasma contacts directly with the catalyst, leading to the previously presented plasma-induced enhancement of adsorption capacity of the zeolite. This way higher carbon dioxide conversions are achieved and due to the adsorption enhancement, higher amounts of the dissociated  $\text{CO}_2$  are hydrogenated into  $\text{CH}_4$ .



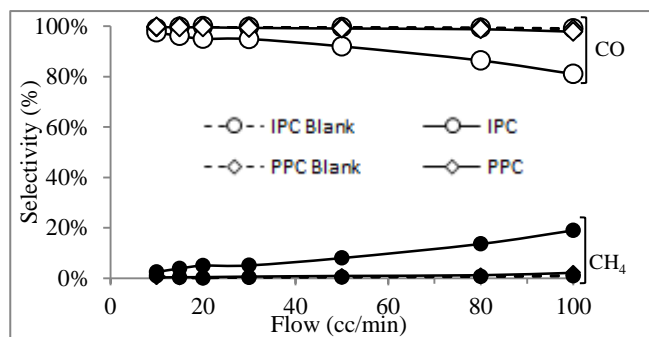


Figure 11 – Product selectivity vs flow results for IPC and PPC.

#### 4. Conclusions

The characterization of Ni-based zeolite catalysts prepared with different impregnation methods, Ni content, Si/Al molar ratios and framework type revealed that the  $\text{Ni}^{2+}$  content of the zeolite, which is related with the alumina content of its framework, affects properties such as the pore volume and the superficial area of the catalyst sample. All these characteristics have their values decreased as the  $\text{Ni}^{2+}$  content in the catalyst increases. The analyzed catalysts exhibit an order of increasing pore size volume and superficial area of:

$$5\% \text{Ni/ZSM-11} < 2.5\% \text{Ni/ZSM-11} < \text{USY(30)} < \text{USY(40)}$$

It was verified that this order inverts if we classify the catalysts by  $\text{Ni}^{2+}$  amount.

The SEM images revealed that USY catalysts have a crystal size of approximately 500 nm while those of the ZSM-11 samples present 250 nm. Nickel Oxide agglomerates were observed and found to be proportional to the Ni content of each catalyst.

The *in-situ*  $\text{H}_2$ TPR-MS experiments performed for the catalyst samples revealed that the catalysts  $\text{Ni}^{\circ}_{\text{frac}}$  increases according with:

$$5\% \text{Ni/ZSM-11} < 2.5\% \text{Ni/ZSM-11} < \text{USY(30)} < \text{USY(40)} < \text{USY(40) (IWI)}$$

The incipient wetness impregnation method was found to allow better dispersion of the Ni particles on the catalysts surface, creating more easily accessible NiO to the reduction and favoring greater  $\text{Ni}^{\circ}_{\text{frac}}$  values.

An estimative of the nickel species present in each catalyst was done, suggesting that, after the catalysts reduction, in USY samples the metal is present under the form of metallic nickel ( $\text{Ni}^{\circ}$ ), nickel ions ( $\text{Ni}^{2+}$ ) and unreduced nickel oxides (NiO). The ZSM-11 samples were found to have nickel only under the form of  $\text{Ni}^{\circ}$  and  $\text{Ni}^{2+}$ .

The catalytic tests performed in the packed-bed reactor revealed that, under conventional heating, the  $\text{CO}_2$  conversion is strongly related with the reduced Ni amount on the surface of the catalyst. The USY catalysts, due to their higher nickel content and reduced fraction, revealed a

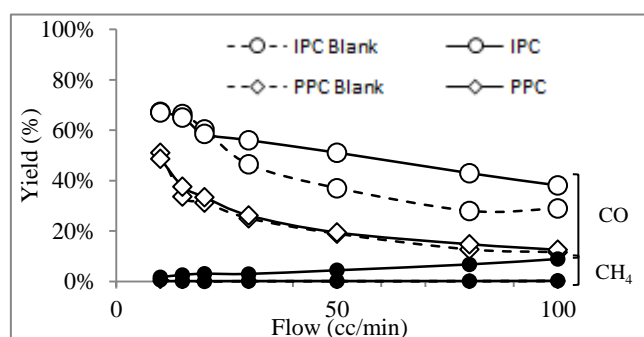


Figure 12 – Product yield vs flow results for IPC and PPC.

higher amount of  $\text{Ni}^{\circ}$  and, therefore, higher carbon dioxide conversions. USY(40) (IWI) presented the highest  $\text{Ni}^{\circ}_{\text{frac}}$  values which justify achieving the best conversion (48% at 450°C), followed by USY(40) (34% at 450°C) and USY(30) (28% at 450°C). Between the two ZSM-11 samples, due to the very low amount of reduced Ni of 5%Ni/ZSM-11, its results were found to be the lowest, only achieving some conversion at very low values after 400°C with a maximum of 3% at the highest temperature. The 2.5%Ni/ZSM-11, despite of having the lowest Ni content of all the studied samples revealed  $\text{CO}_2$  conversion values very close to the ones obtained with USY(30) that has a wt.% of Ni more than 5 times greater than that of this first sample. Based on these results it may be assumed that the MEL structure allows greater activity with less Ni content than that of the faujasites. The conventional heating conversion values achieved with USY(40)(IWI) after 400°C are very close to the ones thermodynamically calculated for these working conditions. The  $\text{Ni}^{\circ}$  content of the catalysts was also related with the selectivity of the reaction under conventional heating. Higher  $\text{Ni}^{\circ}$  amounts allow greater adsorption of hydrogen that facilitates the hydrogenation of the  $\text{CO}$ , which is originated by the dissociation of  $\text{CO}_2$ , into  $\text{CH}_4$ . The methane selectivity under these operating conditions revealed its maximum at 350°C. After this temperature the high temperature, associated to the vacuum, leads to desorption of the species in the catalyst causing a drop in  $\text{CH}_4$  formation. When the reaction is performed under plasma-assistance the  $\text{CO}_2$  values increase from a maximum of 48%, achieved with USY(40) (IWI), to values between 60 and 70% at temperatures between 125 and 350°C, instead of the previous 450°C. After 300°C these values surpass the thermodynamical limit for  $\text{CO}_2$  conversion. Under plasma activity, the formation of highly energized species due to the electric discharge allows breaking these limits and reach conversions that would not be obtained with sole thermal activity. Unlike the conversion of carbon dioxide, when NTP is applied to the reaction  $\text{CH}_4$  selectivity decreases considerably. On the other hand, the  $\text{CO}$  selectivity increases, which can also be interesting in an

industrial point of view. The plasma assisted hydrogenation of CO<sub>2</sub> allows the formation of CO with a very high selectivity and relatively lower temperatures (125°C) than the ones necessary under conventional heating for fulfilling the same objective (450°C).

The blank experiment under plasma activity revealed CO<sub>2</sub> conversion values comparable to the ones obtained with catalyst, suggesting that the dissociation of this compound under plasma occurs in the gas phase without significant influence of the catalyst. However the CO selectivity was above 99%, revealing the catalysts importance in the methane formation under plasma.

A phenomenon of methane storage during plasma activity and its release upon discharge extinction was verified. This was related with an effect of plasma-induced enhancement of the adsorption capacities of the zeolite. This effect is greater for materials that possess higher complex permittivity values. USY catalysts were found to be more affected, in this way, by the NTP discharge than the ZSM-11 catalysts, revealing greater amounts of released methane as well as more selectivity towards this product since, higher adsorption capacity was related with greater hydrogenation of CO into CH<sub>4</sub>. This phenomenon was evidenced by infrared spectroscopy measurements which revealed the adsorption of CH<sub>4</sub> in the catalyst during plasma activity.

After taking the released CH<sub>4</sub> into account for the selectivity and yield calculations it was found that an average amount of 44% of methane is trapped in the catalyst during plasma activity. The CH<sub>4</sub> yield of the plasma-assisted reaction was found to increase from 4% to 6% for the optimal temperature of the most active catalyst. With the released amount of CH<sub>4</sub> all the catalysts excluding the most active reveal methane yield values under plasma (at 200°C) that match or surpass the ones obtained at the optimal temperature obtained for conventional heating (400°C).

From the IPC vs PPC study it was possible to conclude that the residence time of the reactional mixture in plasma is also a major importance factor which can affect not only the amount of converted CO<sub>2</sub> but also the reactional mechanism by sending plasma-excited species into the catalyst before the end of their lifetimes. These results suggest that further enhancement in the CO<sub>2</sub> hydrogenation into CO or methanation may be achieved by optimizing simple parameters such as distance between the electrodes, volumetric flow or reactors diameter.

The plasma-assisted CO<sub>2</sub> hydrogenation proofs to be more energy-efficient than the reaction under conventional heating. Interesting results were achieved for both CO and

CH<sub>4</sub> production. The methane trapping and release may be very promising for the methanation of CO<sub>2</sub> under plasma. Further study about the excited species formed with plasma, their lifetimes, and the reactional path for the production of CH<sub>4</sub> as well as better understanding of the plasma-catalyst interactions or methane trapping capacity can lead the way into taking advantage of these phenomena in order to increase the yield of the reaction towards this product and reaching an even more energy-efficient solution.

## Acknowledgments

The author would like to show his gratitude to the LCS laboratory as well as ENSICAEN and IST for making the internship that led to this master thesis' work possible. To the LCS personnel for the technical support and scientific advises. At last, a particular word of gratitude to Dr. Carlos Henriques, Dr. Federico Azzolina-Jury and Dr. Frédéric Thibault-Starzyk for all the supervision and knowledge that was shared throughout this study.

## References

- [1] REN21, "Renewables 2012 Global Status Report 2012," p. 172, 2012
- [2] E. Jwa, S.B. Lee, H.W. Lee, Y.S. Mok, *Fuel Process. Technol.* 108 (2013) 89-93
- [3] S. Tada, O.J. Ochieng, R. Kykuchi, T. Haneda, H. Kameyama, *Int. J. Hydrogen Energy* 39 (2014) 10090-10100.
- [4] B. Liu, S. Ji, *J. Energy Chemistry* 22 (2013) 740-746
- [5] S. Hwang, J. Lee, U. G. Hong, *J. Ind. Eng. Chem.*, vol. 17, no. 1, pp. 154-157, 2011
- [6] S. Rahmani, M. Rezaei, F. Meshkani, *J. Ind. Eng. Chem.*, vol. 20, no. 4, pp. 1346-1352, 2014
- [7] A. Westermann, B. Azambre, M. C. Bacariza, *Appl. Catal. B Environ.*, vol. 174-175, pp. 120-125, 2015
- [8] P. A. U. Aldana, F. Ocampo, K. Kobl, *Catal. Today*, vol. 215, pp. 201-207, 2013
- [9] F. Azzolina Jury and F. Thibault-Starzyk, "Plasma effects on CO<sub>2</sub> hydrogenation over Ni-based zeolites under high vacuum", Unpublished work
- [10] I. Graça, L. V. González, M. C. Bacariza, *Appl. Catal. B Environ.*, vol. 147, pp. 101-110, 2014.
- [11] M.E. Dry, *Catal. Today* 71 (2002) 227-241.
- [12] M. Magureanu and P. Lukes, *Plasma Chemistry and Catalysis in Gases and Liquids*. 2013